Inorganic Chemistry

Article

pubs.acs.org/IC

Probing the Presence of Multiple Metal−Metal Bonds in Technetium Chlorides by X-ray Absorption Spectroscopy: Implications for Synthetic Chemistry

Frederic Poineau,*[,†] Erik V. Johnstone,[†] Paul M. Forster,[†] Longzou Ma,[‡] Alfred P. Sattelberger,[†,§] and Kenneth R. Czerwinski[†]

[†]Department of Chemistry and [‡]Harry Reid Center for Environmental Studies, University of Nevada Las Vegas, Las Vegas, Nevada 89154, United States

[§]Energy Engineering and Systems Analysis Directorate, Argonne National Laboratory, 9700 South Cass Avenue, Lemont, Illinois 60439, United States

Supporting Information

ABSTRACT: The cesium salts of $[Tc_2X_8]^{3-}$ (X = Cl, Br), the reduction product of $(n\text{-}Bu_4N)[TcOCl_4]$ with $(n\text{-}Bu_4N)BH_4$ in THF, and the product obtained from reaction of $Tc_2(O_2CCH_3)_4Cl_2$ with HCl(g) at 300 °C have been characterized by extended X-ray absorption fine structure (EXAFS) spectroscopy. For the $[Tc_2X_8]^{3-}$ anions, the Tc−Tc separations found by EXAFS spectroscopy (2.12(2) Å for both X = Cl and Br) are in excellent agreement with those found by single-crystal X-ray diffraction (SCXRD) measurements (2.117[4] Å for X = Cl and 2.1265(1) Å for X = Br). The Tc−Tc separation found by EXAFS in these anions is slightly shorter than those found in the $[Tc_2X_8]^{2-}$ anions (2.16(2) Å for X = Cl and Br). Spectroscopic and SCXRD characterization of the reduction product of $(n\text{-}Bu_4N)[TcOCl_4]$ with $(n\text{-}Bu_4N)BH_4$ are consistent with the presence of dinuclear species that are related to the $[Tc_2Cl_8]^{n-}$ (n = 2, 3) anions. From these results, a new preparation of $(n\text{-}Bu_4N)_2[Tc_2Cl_8]$ was developed. Finally, EXAFS characterization of the product obtained from reaction of $Tc_2(O_2CCH_3)_4Cl_2$ with HCl(g) at 300 °C indicates the presence of amorphous α-$TcCl_3$. The Tc−Tc separation (i.e., 2.46(2) Å) measured in this compound is consistent with the presence of Tc═Tc double bonds in the $[Tc_3]^{9+}$ core.

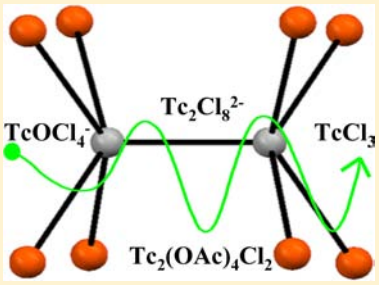

INTRODUCTION

Transition metal compounds with metal−metal multiple bonds play an important role in inorganic, materials, bioinorganic, and organometallic chemistry.[1a−d] These compound bonds can be found in various dimensionalities: molecular clusters (i.e., di-, tri-, tetranuclear species, etc.) and solids with extended structures (i.e., extended metal atom chains and binary halides).[2] More than 4000 dinuclear complexes and several binary halides with metal−metal multiple bonds have been characterized. Multiple bonds between metal atoms were first identified in the rhenium complexes $[Re_3Cl_{12}]^{3-}$ and $[Re_2Cl_8]^{2-}$.[3a,b] An unsupported rhenium−rhenium quadruple bond is present in $[Re_2Cl_8]^{2-}$, while Re═Re double bonds are present in $[Re_3Cl_{12}]^{3-}$. The $(n\text{-}Bu_4N)_2[Re_2Cl_8]$ salt can be obtained by several methods, but the highest yields are obtained from treatment of $(n\text{-}Bu_4N)[ReO_4]$ with refluxing benzoyl chloride, followed by reaction with ethanolic HCl.[4] The $Cs_3[Re_3Cl_{12}]$ salt is obtained from dissolution of Re_3Cl_9 in concentrated HCl followed by precipitation with CsCl. Rhenium trichloride and $(n\text{-}Bu_4N)_2[Re_2Cl_8]$ have been used as precursors for synthesis of polynuclear complexes and contributed significantly to development of rhenium metal−metal bond chemistry.[2d,5] Currently, more than 50 complexes exhibiting the triangular $[Re_3]^{9+}$ core and approximately 550 dinuclear Re complexes with multiple metal−metal bonds have been characterized.

One element whose metal−metal bond chemistry is not well developed is technetium, the lighter rhenium congener. As of 2005, the number of complexes with multiple Tc−Tc bonds was quite limited: 25 dinuclear species and 4 hexanuclear and 6 octanuclear halide clusters had been structurally characterized;[6] no Tc binary halides with multiple Tc−Tc bonds and no complexes with a $[Tc_3]^{9+}$ core were reported prior to 2006. For the past 6 years, we have focused on expanding the chemistry of dinuclear complexes and identifying new binary halides of technetium.

Recent studies of dinuclear species with $[Tc_2]^{n+}$ (n = 4, 5, 6) cores gave valuable information on the nature of the Tc−Tc bonding in these compounds.[7a−c] Multiple Tc−Tc bonded dinuclear species exhibit bond orders (BO) of 4, 3.5, and 3. The bond order is defined as $BO = (n_b - n_a)/2$, where n_b and n_a designate the number of electrons in bonding and antibonding orbitals, respectively. Quadruply bonded technetium dinuclear species exhibit Tc−Tc separations in the range 2.16−2.19 Å, while separations in the range 2.09−2.15 Å are observed for

Received: July 9, 2012
Published: August 20, 2012

dx.doi.org/10.1021/ic3014859 | Inorg. Chem. 2012, 51, 9563−9570

complexes with BOs of 3 and 3.5.[6] The Tc−Tc separations in the quadruply bonded Tc complexes are longer than in the triply bonded ones. This phenomenon has been analyzed recently via theoretical calculations; the results show that a stronger π bond in $[Tc_2X_8]^{3-}$, relative to $[Tc_2X_8]^{2-}$, is the origin of the shorter Tc−Tc separation in the $[Tc_2X_8]^{3-}$ complexes.[7b,c]

In our studies on quadruply bonded technetium complexes we have shown that EXAFS spectroscopy yields Tc−Tc separations that are in good agreement with the SCXRD results.[8] Complexes with bond orders of 3.5 represent a large subgroup of metal−metal-bonded technetium dinuclear species, but their structures have not yet been probed by EXAFS spectroscopy. The study of the $[Tc_2X_8]^{3-}$ anions (X = Cl, Br) by EXAFS will further benchmark the efficacy and accuracy of this technique for measuring Tc−Tc separations. EXAFS spectroscopy can also be used as a tool to better understand and optimize the synthesis of $(n\text{-}Bu_4N)_2[Tc_2Cl_8]$ and Tc_3Cl_9, two important precursors in Tc metal−metal-bonded chemistry.

The compound $(n\text{-}Bu_4N)_2Tc_2Cl_8$ was unambiguously identified in 1980,[9] and it has been claimed by several different methods.[10] The method that produces the highest yield is a multistep procedure requiring 2−3 days. The first step is the reduction of the technetium(V) salt $(n\text{-}Bu_4N)[TcOCl_4]$ with 2 mol of $(n\text{-}Bu_4N)BH_4$ in THF followed by precipitation of an oily brown solid with ether.[8a,10a]Subsequent treatment of the sticky solid with aqueous HCl in acetone produces $(n\text{-}Bu_4N)_2[Tc_2Cl_8]$ in ∼30% yield. The composition of the brown solid is unclear, and various hypotheses can be advanced, e.g., a Tc−THF adduct such as $[TcCl_3(THF)_3]$, a dinuclear species (i.e., $(n\text{-}Bu_4N)_x[Tc_2Cl_{6+x}]$; x = 0, 1, 2), or solids with extended structures possibly related to $K_2[Tc_2Cl_6]$.[6] In order to get structural information on this key intermediate and better understand the synthesis of $(n\text{-}Bu_4N)_2[Tc_2Cl_8]$, EXAFS characterization of the brown solid was pursued.

In our study on Tc binary chlorides, we synthesized two polymorphs of the trichloride: α-$TcCl_3$ and β-$TcCl_3$.[11a,b] The compound α-$TcCl_3$ (Tc_3Cl_9) is isostructural to Re_3Cl_9 and consists of triangular Tc_3Cl_9 clusters, while β-$TcCl_3$ is isostructural to $MoCl_3$ and $RuCl_3$ and consists of infinite layers of edge-sharing $TcCl_6$ octahedra. First-principles calculations indicate that both trichlorides possess Tc═Tc double bonds. The compound β-$TcCl_3$ was obtained congruently with $TcCl_2$ from reaction of Tc metal and Cl_2(g) in a sealed tube at 450 °C.[10b,c] Formation of α-$TcCl_3$ was reported in three different reactions: thermal annealing of β-$TcCl_3$ at 280 °C over several weeks, decomposition of $TcCl_4$ under vacuum at 450 °C, and the reaction between $Tc_2(O_2CCH_3)_4Cl_2$ and HCl(g) at 300 °C followed by sublimation in a sealed tube.[12] The flowing gas reaction is the method of choice for production of weighable amounts of α-$TcCl_3$. The black powder obtained from the reaction between $Tc_2(O_2CCH_3)_4Cl_2$ and HCl(g) at 300 °C was X-ray amorphous. By analogy with the corresponding rhenium reaction, this powder was assumed to be α-$TcCl_3$ but no analyses were performed.[13] The recent discovery of β-$TcCl_3$ and its conversion to α-$TcCl_3$ may indicate that this powder could also be β-$TcCl_3$. For future uses of α-$TcCl_3$ in synthetic chemistry, characterization of the powder formed at 300 °C is necessary.

The work presented here consists of three parts: (A) characterization of the $[Tc_2X_8]^{3-}$ cesium salts (X = Cl, Br) by EXAFS spectroscopy; (B) characterization of the reduction product of $(n\text{-}Bu_4N)[TcOCl_4]$ with $(n\text{-}Bu_4N)BH_4$ in THF and development of a new procedure for the preparation of $(n\text{-}Bu_4N)_2[Tc_2Cl_8]$; (C) characterization of the product obtained from reaction of $Tc_2(O_2CCH_3)_4Cl_2$ with HCl(g) at 300 °C.

EXPERIMENTAL SECTION

Caution! *Techetium-99 is a weak beta emitter (E_{max} = 292 keV). All manipulations were performed in a radiochemistry laboratory at UNLV designed for chemical synthesis with radionuclides using efficient HEPA-filtered fume hoods and following locally approved radioisotope handling and monitoring procedures. The starting compound $NH_4[TcO_4]$ was purchased from Oak Ridge National Laboratory and purified as described elsewhere.*[11a]

A. Preparation of Compounds. Compounds $(n\text{-}Bu_4N)[TcOCl_4]$, $Tc_2(O_2CCH_3)_4Cl_2$, and the cesium salt of $[Tc_2Br_8]^{3-}$ were prepared according the methods reported in the literature.[7b,8a,b]

The $[Tc_2Cl_8]^{3-}$ cesium salt was prepared using a method similar to the one used for the bromide analogue; the synthesis involves disproportionation of $(n\text{-}Bu_4N)_2[Tc_2Cl_8]$ in warm concentrated HCl(aq), followed by selective precipitation of the $[TcCl_6]^{2-}$ and $[Tc_2Cl_8]^{3-}$ anions with CsCl (SI 1, Supporting Information). The $[Tc_2X_8]^{3-}$ cesium salts were characterized by UV−vis and X-ray absorption near edge structure (XANES) spectroscopy.[14]

Preparation of $(n\text{-}Bu_4N)_2[Tc_2Cl_8]$. The compound was prepared by two methods: the first method (method a) has been described in detail in the literature,[8a] while method b has been developed in the current work. For both methods, reactions were performed in a 250 mL round-bottom flask equipped with 3-hole rubber stopper.

Method a. The compound $(n\text{-}Bu_4N)[TcOCl_4]$ was dissolved in THF and reduced with $(n\text{-}Bu_4N)BH_4$. After reduction, ether was added to the brown solution and a dark solid was observed at the bottom of the flask. The supernatant was removed and the solid pumped to dryness forming a sticky brown solid **1**. After treatment of **1** with acetone:HCl(aq) and recrystallization, the $(n\text{-}Bu_4N)_2[Tc_2Cl_8]$ salt was obtained in a ∼36% yield. $(n\text{-}Bu_4N)_2[Tc_2Cl_8]$ was analyzed by EXAFS spectroscopy (Figure S1 and Table S1, Supporting Information) and used for preparation of $Tc_2(O_2CCH_3)_4Cl_2$ and the $[Tc_2X_8]^{3-}$ (X = Cl, Br) cesium salts. A portion (∼ 20 mg) of the solid **1** was separated and used for EXAFS measurement (Results and Discussion). Additional details are presented in SI 2, Supporting Information.

Method b. $(n\text{-}Bu_4N)[TcOCl_4]$ (933 mg 1.866 mmol) was dissolved in THF (20 mL). A solution of $(n\text{-}Bu_4N)BH_4$ (967 mg, 3.764 mmol) in THF (20 mL) was added under a countercurrent of Ar. Five minutes after addition, the brown supernate was removed with a pipet and a brown solid was observed at the bottom of the flask. The solid was washed with THF (2 × 10 mL) and ether (2 × 10 mL). After washing, the brown solid turned yellow-green (solid **2**) and was dried under an Ar stream. Then, CH_2Cl_2 (20 mL) was added to the flask, the solution was stirred, and an HCl(g) stream was passed slowly through the solution for 7 min. A change of color from yellow-green to emerald-green occurred immediately. Hexane (20 mL) was added to the flask, and a green solid precipitated. The supernatant was removed by pipet, and the crude $(n\text{-}Bu_4N)_2[Tc_2Cl_8]$ was washed with hexane (20 mL) and dried with an Ar stream. Acetone (20 mL) was added to the flask, the green solution was transferred into four centrifuged tubes, and $(n\text{-}Bu_4N)_2[Tc_2Cl_8]$ recrystallized by adding a minimal amount of ether to each tube. After centrifugation, removal of the supernates, and drying with an Ar stream, $(n\text{-}Bu_4N)_2[Tc_2Cl_8]$ (333 mg, 0.345 mmol) was isolated; yield = 37%, based on $(n\text{-}Bu_4N)[TcOCl_4]$.

Reaction between $Tc_2(O_2CCH_3)_4Cl_2$ and HCl(g) at 300 °C. Reaction was performed using the method previously described.[10a] A weighted quantity (34 mg, 0.067 mmol) of $Tc_2(O_2CCH_3)_4Cl_2$ was dispersed in a 3 in. quartz boat which was then placed in a long quartz tube equipped with 25 mm Solv-Seals at each end. The entire apparatus was placed in a clamshell tube furnace and purged with HCl(g). The temperature was raised to 300 °C (10 °C/min) and held there for 2 h, after which the system was cooled to room temperature.

dx.doi.org/10.1021/ic3014859 | Inorg. Chem. 2012, 51, 9563−9570

Some volatilization of the intermediate $Tc_2(O_2CCH_3)_2Cl_4$ occurred between 175 and 250 °C. After reaction, 21.3 mg of a black powder **3** remained in the boat. X-ray diffraction powder measurement shows **3** to be amorphous, and its infrared spectrum is devoid of any vibrational modes indicative of acetate ligands. The Tc content in **3** is consistent with $TcCl_3$. Anal. Calcd for $TcCl_3$: Tc, 48.2. Found: Tc, 47.3. Yield = 77%.

B. Characterization Techniques. *EXAFS Spectroscopy.* Measurements were performed at the Argonne National Laboratory Advanced Photon Source at the BESSRC-CAT 12 BM-B station.[15] Solid **1** was diluted 5% in mass in boron nitride (BN), while all the other solids were diluted at 1% in BN. Samples were placed in an aluminum sample holder equipped with Kapton windows. For samples diluted at 1%, EXAFS spectra were recorded at the Tc−K edge (21 044 eV) in fluorescence mode at room temperature using a 13-element germanium detector. For solid **1**, the EXAFS spectrum was recorded in transmission mode. A double crystal of Si [111] was used as a monochromator. Rejections of harmonics were performed using rhodium mirrors. The energy was calibrated using a molybdenum foil. Fourteen scans were recorded in the k range 0−15 $Å^{-1}$ and averaged. EXAFS spectra were extracted using the Athena[16] software, and data analysis was performed using Winxas.[17] For the fitting procedure, amplitude and phase shift functions were calculated by FEFF 8.2.[18] Input files were generated by Atoms.[19] Adjustments of the k^3-weighted EXAFS spectra were under the constraints $S_0^2 = 0.9$.

Other Techniques. Single-crystal X-ray diffraction data were collected on a Bruker Apex II system equipped with an Oxford nitrogen cryostream operating at 100 K. Crystals were mounted under Paratone on a glass fiber. Data processing was performed using the Apex II suite, and refinements were carried out using SHELX97 and OLEXII.[20a,b] UV−vis spectra were performed at room temperature in a quartz cell (1 cm) on a Cary 6000i double-beam spectrometer. Samples were dissolved in CH_2Cl_2, which was also used as the reference. Attenuated total reflectance Fourier transform infrared (ATR-FTIR) measurements were performed on a Varian Excalibur spectrometer using a KBr beam splitter and an integrated Durasampler diamond ATR. Energy-dispersive X-ray (EDX) spectroscopy measurements were performed on a TECNAI-G2-F30 Supertwin transmission electron microscope with a 300 keV field emission gun; samples were prepared by grinding the compound with hexane in an agate mortar, taking one drop of the solution and placing it onto a 3 mm diameter carbon film supported on a copper grid. For elemental analyses, the compounds were diluted in concentrated HCl (10 mL) and the solution warmed (100 °C) for 1 h. After cooling to room temperature, the Tc concentration was determined by UV−vis spectroscopy using the absorbance at 340 nm of the $[TcCl_6]^{2-}$ anion.[21]

RESULTS AND DISCUSSION

A. EXAFS Study of $[Tc_2X_8]^{3-}$ (X = Cl, Br) Cesium Salts. The extracted EXAFS spectra of the $[Tc_2X_8]^{3-}$ cesium salts (X = Cl, Br) were k^3-weighted and the Fourier transformation (FT) done in the k range 2.5−14 $Å^{-1}$ for X = Cl and 3.5−14 $Å^{-1}$ for X = Br. EXAFS spectra were adjusted using the scattering functions calculated from the crystallographic structure of $[Cs_{(2+x)}][H_3O_{(1-x)}][Tc_2Br_8]\cdot 4.6\ H_2O$ and $K_3[Tc_2Cl_8]\cdot 2H_2O$.[7b,22] These scattering functions involve the Tc and halide atoms located in the first coordination shell (Tc1 and X1) and the halide in the second coordination shell (Figure 1). For the adjustments, ΔE_0 was constrained to be the same value for each wave and the numbers of atoms were fixed at those of the crystal structure; all other parameters were allowed to vary.

For $[Tc_2Br_8]^{3-}$, the results of the adjustment (Figure 2, Table 1) indicate that the environment of the absorbing atom consists of a second Tc atom at 2.12(2) Å and Br atoms at 2.51(3) and 3.72(4) Å. These distances are in good agreement with the ones reported by SCXRD measurements (Table 2).

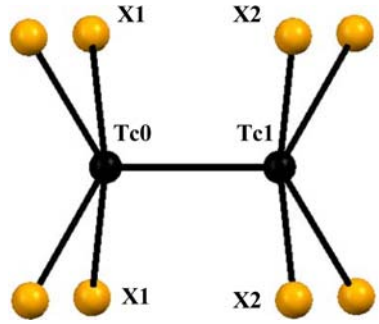

Figure 1. Ball and stick representation of the $[Tc_2X_8]^{3-}$ (X = Cl, Br) anions. Tc and X atoms are in black and yellow-orange, respectively. Tc0 represents the absorbing atom.

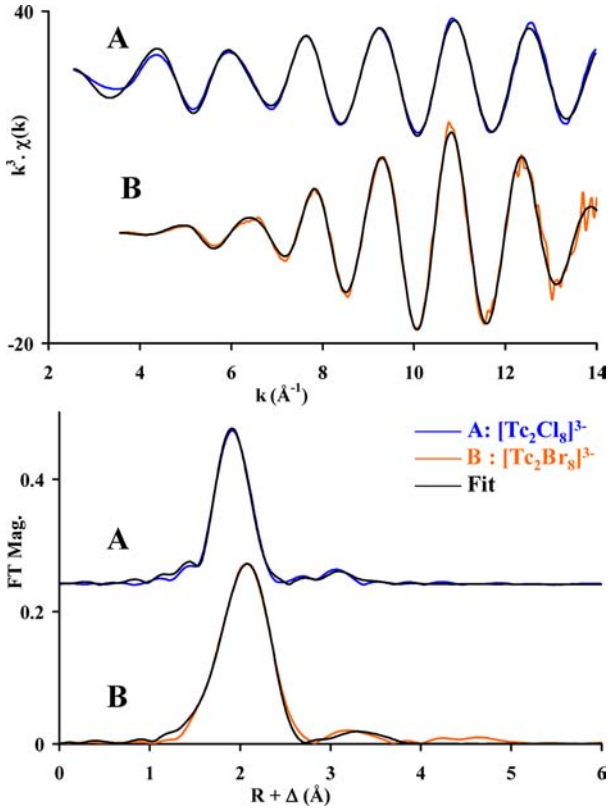

Figure 2. Fitted experimental k^3 EXAFS spectra (top) and Fourier transform of k^3 EXAFS spectra (bottom) of (A) $[Tc_2Cl_8]^{3-}$ and (B) $[Tc_2Br_8]^{3-}$. Adjustment performed between k = 2.5 and 14 $Å^{-1}$ for $[Tc_2Cl_8]^{3-}$ and 3.5 and 14 $Å^{-1}$ for $[Tc_2Br_8]^{3-}$. Experimental data are in blue for X = Cl and in orange for X = Br. Fits are in black.

Table 1. Structural Parameters Obtained by Adjustment of the k^3 EXAFS Spectra of $[Tc_2X_8]^{3-}$ (X = Cl, Br)[a]

complex	scattering	CN	R (Å)	σ^2 (Å^2)
$[Tc_2Br_8]^{3-}$	Tc0 ⇆ Tc1	1	2.12(2)	0.0021
	Tc0 ⇆ Br1	4	2.51(2)	0.0031
	Tc0 ⇆ Br2	4	3.72(4)	0.0125
$[Tc_2Cl_8]^{3-}$	Tc0 ⇆ Tc1	1	2.12(2)	0.0022
	Tc0 ⇆ Cl1	4	2.38(2)	0.0033
	Tc0 ⇆ Cl2	4	3.62(4)	0.0122

[a] ΔE_0 (eV) = 2.56 for X = Cl and 1.07 for X = Br. $S_0^2 = 0.9$.

For $[Tc_2Cl_8]^{3-}$, the results of the adjustment (Figure 2, Table 1) indicate that the environment of the absorbing atom

dx.doi.org/10.1021/ic3014859 | Inorg. Chem. 2012, 51, 9563−9570

Table 2. Interatomic Distances (Å) Found by EXAFS Spectroscopy, SCXRD Measurements (bold), and Raman Spectroscopy (italics) in the $[Tc_2X_8]^{n-}$ (n = 2, 3) and $Tc_2(O_2CCH_3)_4X_2$ (X = Cl, Br) Complexes[7a,b,8b]

complex	Tc−Tc	Tc−X	complex	Tc−Tc	Tc−X
$[Tc_2Cl_8]^{2-}$	2.16(2)	2.34(2)	$[Tc_2Cl_8]^{3-}$	2.12(2)	2.38(2)
	2.1560(3)	**2.3223(8)**		**2.117(4)**	**2.363(15)**
$[Tc_2Br_8]^{2-}$	2.16(2)	2.48(2)	$[Tc_2Br_8]^{3-}$	2.12(2)	2.51(2)
	2.1635(9)	**2.473(2)**		**2.1265(10)**	**2.515(2)**
$Tc_2(O_2CCH_3)_4Cl_2$	2.18(2)	2.43(2)	$Tc_2(O_2CCH_3)_4Br_2$	2.19(2)	2.63(3)
	2.192	*2.408*		*2.192*	*2.60*

consists of a second Tc atom at 2.12(2) Å and Cl atoms at 2.38(2) and 3.62(4) Å. The crystallographic structure of the $[Tc_2Cl_8]^{3-}$ cesium salt is unknown, but the interatomic distances found in the $[Tc_2Cl_8]^{3-}$ anion are in good agreement with those found by SCXRD measurements for other $[Tc_2Cl_8]^{3-}$ salts.[6]

In summary, for a single-phase (i.e., pure) sample, the structural parameters measured by EXAFS spectroscopy in metal−metal multiply bonded dinuclear species agree quite satisfactorily with the ones found by SCXRD (Table 2). For a mixture of compounds with various Tc−Tc separations, the resolution of EXAFS under our experimental conditions ($\pi/2\Delta k$ = 0.136 Å) would allow us to separate the Tc−Tc contributions of compounds that exhibit Δ(Tc−Tc) > 0.136 Å. A value of Δ(Tc−Tc) > 0.136 Å is observed for the Tc binary chlorides: $TcCl_4$ (Tc−Tc = 3.6048(3) Å), α-$TcCl_3$ (Tc−Tc = 2.444(1 Å), β-$TcCl_3$(Tc−Tc = 2.861(1) Å), and $TcCl_2$ (Tc−Tc = 2.127(2) Å).[11a−c] A limitation of EXAFS appears for mixtures of Tc−Tc-bonded dinuclear species where Δ(Tc−Tc) is lower than 0.136 Å; the difference between the longest and the shortest Tc−Tc separation in multiple-bonded dinuclear species is 0.098(2) Å.[6] For a mixture, EXAFS would not separate the individual Tc−Tc contributions, and the measured Tc−Tc distances would represent an average value.

In the following sections, EXAFS will be used to probe the presence of metal−metal bonds in the reduction product of (n-Bu_4N)[$TcOCl_4$] with (n-Bu_4N)BH_4 in THF, as well as in the product obtained from the reaction of $Tc_2(O_2CCH_3)_4Cl_2$ with HCl(g) at 300 °C.

B. Study of the Reduction Product of (n-Bu_4N)[$TcOCl_4$] with (n-Bu_4N)BH_4 in THF. The oily brown solid **1** formed after reduction of (n-Bu_4N)[$TcOCl_4$] with (n-Bu_4N)BH_4 (Method a) was analyzed by EDX and EXAFS spectroscopy. Analysis by EDX spectroscopy reveals the presence of C, Tc, Cl, and O atoms in the sample (Figure S3A, Supporting Information). Concerning the analysis by EXAFS spectroscopy, the extracted EXAFS spectrum was k^3-weighted and the Fourier transformation (FT) done in the k range 2.5−14 $Å^{-1}$.

The FT (Figure 3) exhibits one main peak located at $R + \Delta$ = 1.98 Å. No other significant contribution is observed on the FT above this distance, which is consistent with the absence of Tc atoms in the second coordination shell around the absorbing atom. The position of this peak is similar to the one of the $[Tc_2Cl_8]^{n-}$ species (i.e., 1.91 Å for n = 3 and 1.94 Å for n = 2); this indicates that the absorbing Tc atoms in **1** are surrounded by Cl and/or Tc atoms.

Three different adjustments (1, 2, and 3) were performed considering the following: (1) the Tc0Δ ⇆ Cl1 scattering, (2) the Tc0 ⇆ Cl1 and Tc0 ⇆ Tc1 scatterings, and (3) the Tc0 ⇆ Cl1, Tc0 ⇆ Tc1, and Tc0 ⇆ O scatterings. The Tc0 ⇆ Cl1, Tc0 ⇆ Tc1, and Tc0 ⇆ O scattering functions were calculated from the crystallographic structures of (n-Bu_4N)$_2$[Tc_2Cl_8] and

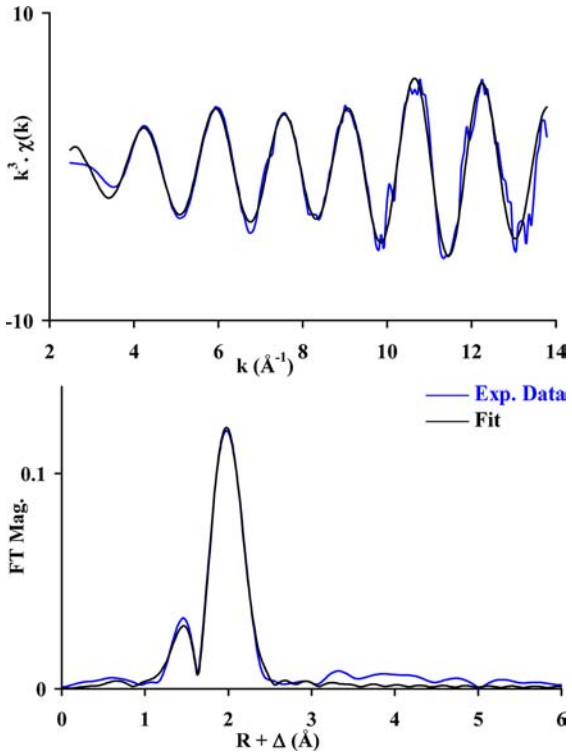

Figure 3. Fits of the experimental k^3 EXAFS spectra (top) and Fourier transform of k^3 EXAFS spectra (bottom) of the oily solid **1**. Adjustment performed between k = 2.5 and 14 $Å^{-1}$. Experimental data are in blue, and the fit is in black.

$NH_4[TcO_4]$.[7b,23] For the adjustments, the value of the Debye−Waller factors (DWF) for the Tc0 ⇆ Cl1 and Tc0 ⇆ Tc1 scatterings were fixed to those determined in (n-Bu_4N)$_2$[Tc_2Cl_8] (i.e., σ^2_{Tc-Cl} = 0.0031 $Å^2$, σ^2_{Tc-Tc} = 0.0029 $Å^2$; Table S1, Supporting Information). For the Tc−O scattering, the value of σ^2_{Tc-O} was fixed to the one determined in K[TcO_4] (i.e., 0.0014 $Å^2$, Figure S2 and Table S2, Supporting Information). ΔE_0 was constrained to be the same value for each wave; all other parameters were allowed to vary. The best adjustment (lower value of the reduced chi^2) was obtained considering the Tc0 ⇆ Cl1, Tc0 ⇆ Tc1, and Tc0 ⇆ O scatterings. The results of the adjustment (Figure 3, Table 3) indicate the environment of the Tc0 atom to be constituted by 0.7(1) Tc atoms at 2.18(2) Å, 2.9(6) Cl atoms at 2.41(2) Å, and 0.3(1) O atoms at 1.74(2) Å.

The number of Tc atoms in the first coordination shell and the Tc−Tc separation are consistent with those found in multiply Tc−Tc-bonded dinuclear complexes. The Tc−Tc separation is similar to the one found for Tc quadruple-bonded dinuclear species (Table 2). We note that the presence of compounds with different bond orders is not excluded.

dx.doi.org/10.1021/ic3014859 | Inorg. Chem. 2012, 51, 9563−9570

Table 3. Structural Parameters Obtained by Adjustment of the k^3 EXAFS Spectra of the Oily Brown solid 1[a]

fit	scattering	CN	R (Å)	σ^2 (Å^2)	reduced chi^2
1	Tc0 ⇆ Cl1	3.0(6)	2.44(3)	0.0029	1432.9
2	Tc0 ⇆ Tc1	0.8(2)	2.19(2)	0.0029	206.2
	Tc0 ⇆ Cl1	3.1(6)	2.41(2)	0.0029	
3	Tc0 ⇆ Tc1	0.7(1)	2.18(2)	0.0029	
	Tc0 ⇆ Cl1	2.9(6)	2.41(2)	0.0031	63.8
	Tc0 ⇆ O	0.3(1)	1.74(2)	0.0014	

[a]Adjustments 1, 2, and 3 performed between k = 2.5 and 14 Å^{-1}. ΔE_0 = 7.1 (1), 3.14 (2), and 6.4 eV (3). S_0^2 = 0.9.

The measured Tc−Cl distance (2.41(2) Å) is larger than those found by EXAFS in the $[Tc_2Cl_8]^{n-}$ anions (Table 2) and in $[TcCl_6]^{2-}$ (2.36(2) Å); rather, it is more consistent with the values found in mononuclear Tc(II) species (i.e., 2.41−2.43 Å).[24] The Tc−O distance (1.74(2) Å) is shorter than the one reported in $[TcCl_4L_2]$ complexes (i.e., Tc−O = 2.096(7) Å for L = H_2O and 2.111(4) Å for L = THF) and larger than the one found in $[TcOCl_4]^-$ (i.e., 1.610(4) Å).[25a−c] This distance is similar to the one found in the $[TcO_4]^-$ anion (1.702(2) Å)[23] or in complexes with a [Tc−O−Tc] core structure (i.e., 1.800(3) Å for ([(Pic)Cl_3(Pic)Tc−O−TcCl(Pic)$_3$Cl]), pic = picoline).[26] Again, we cannot exclude the possibility that **1** contains compounds with various Tc−O and Tc−Cl distances.

In order to isolate the compound(s) containing metal−metal bonds, the solubility of solid **1** was studied in different solvents (ether, hexane, acetone, CH_3CN, THF). Solid **1** is highly soluble in acetone and CH_3CN and insoluble in ether and hexane. Washing **1** with THF leads to a yellow-green solid **2** and brown supernatant (Supporting Information, SI3). During the synthesis of (n-Bu_4N)$_2$[Tc_2Cl_8] (Method b), a careful inspection of the solution obtained immediately after reduction of (n-Bu_4N)[$TcOCl_4$] reveals the presence of solid **2** at the bottom of the flask. Solid **2** was characterized by elemental analysis, spectroscopic (EDX, Infrared, UV−vis), and X-ray diffraction techniques and its reactivity studied in CH_2Cl_2:HCl(g).

Elemental analysis indicates that the Tc content in **2** (i.e., Tc = 0.00177 mmol/mg) is lower than the one in (n-Bu_4N)$_2$[Tc_2Cl_8] (i.e., 0.0021 mmol/mg) and higher than the one in (n-Bu_4N)$_2$[$TcCl_6$] (0.0013 mmol/mg).

Characterization of **2** by EDX spectroscopy (Figure S3B, Supporting Information) shows the sample to contain Tc, Cl, and C atoms, while no O atoms were detected. The IR spectrum (Figure S4, Supporting Information) shows bands at 2877 and 2960 cm^{-1} characteristic of the C−H stretching in the (n-Bu_4N)$^+$ fragment. No bands in the region 1000−1100 cm^{-1} (Tc═O: 1020 cm^{-1}, Figure S5, Supporting Information) were observed, which is consistent with the absence of (n-Bu_4N)[$TcOCl_4$].

The UV−vis spectrum recorded in air after dissolution of **2** in CH_2Cl_2 (Figures 4 and 5, Table 4) exhibits 3 bands in the region 300−700 nm and a large band in the region 1200−1600 nm. Analysis of the UV−vis spectrum of the solution at 25 min intervals (Figure 5) indicates that the large band at 1200−1600 nm is unstable (absorption at 1590 nm decrease by ∼50%), while the band at 676 nm is stable; this result is consistent with the presence of at least two species in solution. The position of the bands at 305, 389, and 676 nm are similar to the ones reported for the $[Tc_2Cl_8]^{2-}$ anion (Table 4). By analogy with $[Tc_2Cl_8]^{2-}$, the band at 676 nm is attributed to the $\delta \rightarrow \delta^*$ transition while the bands at 305 and 389 nm correspond to π(Cl) → δ^* transitions.[8a] The large band at 1200−1600 nm is similar to the one observed in dinuclear species with a $[Tc_2]^{5+}$ core and also attributed to a $\delta \rightarrow \delta^*$ transition.[27] The behavior in CH_2Cl_2 of the species with the bands at 674 and 1200−1600 nm is consistent with previous observation on $[Tc_2X_8]^{n-}$ species (X = Cl, Br; n = 2, 3); it was reported that $[Tc_2X_8]^{2-}$ anions are stable in organic solvents, while $[Tc_2X_8]^{3-}$ rapidly decomposes.[10a]

In order get more information on the complexes present in **2**, the solid was dissolved in acetone:ether (2:1) and CH_2Cl_2:hexane (4:1) and the solutions were placed in a

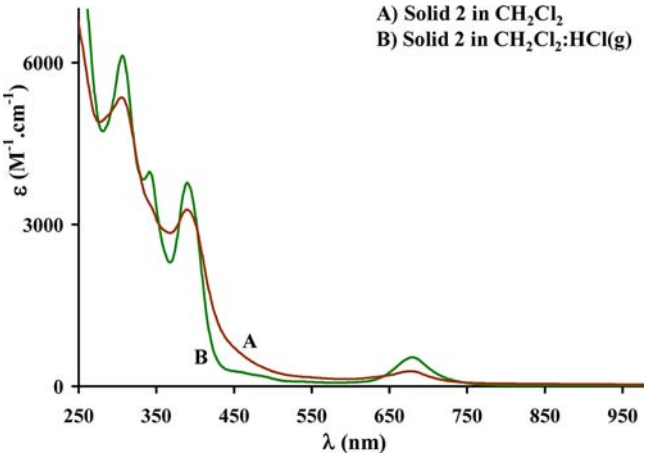

Figure 4. Absorption spectra (250−1000 nm) of the solutions obtained after dissolution of solid **2** in CH_2Cl_2 (A, brown) and CH_2Cl_2:HCl(g) (B, green).

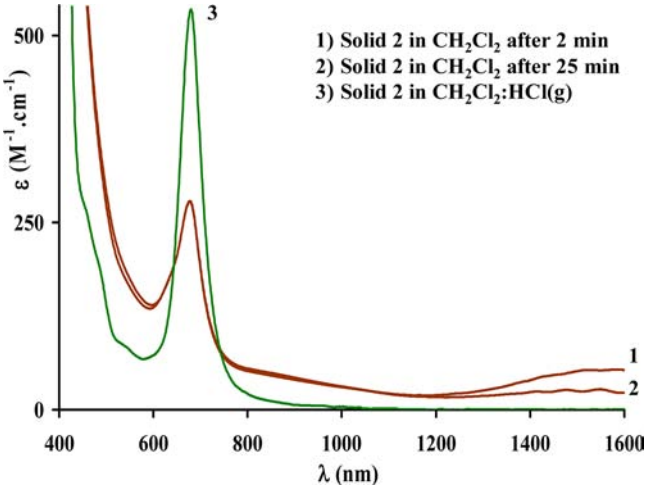

Figure 5. Absorption spectra (400−1600 nm) of solutions obtained after dissolution of solid **2** in CH_2Cl_2 after t = 2 (1) and 25 min (2) and in CH_2Cl_2:HCl(g) (3, green).

Table 4. Wavelength (nm) and Absorption Coefficient (M^{-1}·cm^{-1}) Determined for Solid 2 in CH_2Cl_2 and CH_2Cl_2:HCl(g) and for the $[Tc_2Cl_8]^{2-}$ Anion in CH_2Cl_2

compound	wavelength (nm) (ε_{max} (M^{-1}·cm^{-1}))
solid **2** in CH_2Cl_2	305 (5354), 389 (3276), 676 (281), 1590 (54)
solid **2** in CH_2Cl_2:HCl(g)	306 (6126), 390 (3772), 680(535) and 340 (3975)
$Tc_2Cl_8^{2-}$ in CH_2Cl_2	303 (10564), 390 (8674), 680(1391)

dx.doi.org/10.1021/ic3014859 | Inorg. Chem. 2012, 51, 9563−9570

freezer at −25 °C. From both solutions, emerald green single crystals were obtained after 2 days and analyzed by SCXRD. For crystals obtained from acetone:ether, the compound crystallizes in the monoclinic space group $P2_1/c$ (a = 10.1856(10) Å, b = 14.8529(15) Å, c = 17.2877(18) Å, β = 91.214(2)°). The unit cell contains a technetium anion with a 2− charge (either $[Tc_2Cl_8]^{2-}$ or $[TcCl_6]^{2-}$ as discussed below), $(n\text{-}Bu_4N)^+$ ions, and acetone molecules. The region occupied by the technetium anion is disordered. $[Tc_2Cl_8]^{2-}$ is present primarily (refined occupancy = 90.69(11)%), but some $[TcCl_6]^{2-}$ was found to occupy the site as well (9.31(11)%). Lattice parameters are similar to the ones reported for the $(n\text{-}Bu_4N)_2[Tc_2Cl_8]$ acetone solvate (i.e., a = 10.1601(19) Å, b = 14.838(3) Å, c = 17.398(3) Å, β = 91.345(3)°).[8b] The interatomic Tc−Tc distance found in $[Tc_2Cl_8]^{2-}$ (i.e., 2.1563(4) Å) is identical to the ones previously reported (i.e., 2.1560(3) Å).

For crystals obtained from CH_2Cl_2:hexane, the results indicate the presence of a CH_2Cl_2 solvate. The crystal structure of the CH_2Cl_2 solvate is similar in most respects to the structure described above. The Tc−Tc distance within the $[Tc_2Cl_8]^{2-}$ anion is essentially identical to the one grown in acetone (Tc−Tc = 2.1539[18]). The unit cell is monoclinic ($P2_1/c$) with b and c virtually identical to the previous values (i.e., b = 14.7166(19) Å, c = 16.908(2) Å) but doubled along a (21.815(3) Å). The doubling accommodates two crystallographically unique $[Tc_2Cl_8]^{2-}$ species, two unique $(n\text{-}Bu_4N)^+$ cations, and three dichloromethane molecules. One of the two $(n\text{-}Bu_4N)^+$ cations exhibits positional disorder on a single butyl group; the other does not. Additionally, dichloromethane-solvated crystals are unstable outside of the mother liquor and quickly lose solvent *and* crystallinity even under Paratone. Despite working quickly, some loss of crystallinity is apparent. These two factors contributed to a higher R_1 (7.42%). Formation of $(n\text{-}Bu_4N)_2[Tc_2Cl_8]$ crystals from acetone and CH_2Cl_2 solutions is consistent with the initial presence of the $[Tc_2Cl_8]^{2-}$ anion in the solid **2**.

Solid **2** is highly soluble in CH_2Cl_2, yielding a yellow-green solution that immediately turns to an intense emerald green upon passing HCl(g) through the solution. After acidification, UV−vis spectra (Figure 4 and Figure 5) show a strong enhancement of the absorption coefficients of the bands at 305, 389, and 676 nm; the appearance of a band at 340 nm ($[TcCl_6]^{2-}$) and disappearance of the large band at 1200−1600 nm are also noticed. Deconvolution of the spectra after acidification (Figure S5, Supporting Information) is consistent with the presence of the $[Tc_2Cl_8]^{2-}$ (∼80%) and $[TcCl_6]^{2-}$ anions (∼20%). In a typical experiment (SI 4, Supporting Information), the solid **2** was converted to $(n\text{-}Bu_4N)_2[Tc_2Cl_8]$ in ∼75% yield.

In summary, the EXAFS characterization indicates the presence of Tc−Tc-bonded dimer(s) in the oily solid **1**. Attempts to isolate these dimer(s) from **1** lead to a yellow-green solid **2**. It was noticed that **2** is also directly obtained during reduction of $(n\text{-}Bu_4N)[TcOCl_4]$ by $(n\text{-}Bu_4N)BH_4$.

Characterization of **2** by infrared and EDX spectroscopy are consistent with the presence of the $(n\text{-}Bu_4N)^+$ fragment and with Tc, Cl, and C atoms within the solid. The UV−vis spectrum of **2** in CH_2Cl_2 exhibits bands that are characteristic of complexes with the $[Tc_2]^{6+}$ and $[Tc_2]^{5+}$ cores. The species with the $[Tc_2]^{6+}$ core is stable in CH_2Cl_2 and exhibits a spectrum similar to that of $[Tc_2Cl_8]^{2-}$. The species with the $[Tc_2]^{5+}$ core is highly unstable; its behavior is consistent with the one reported for the $[Tc_2X_8]^{3-}$ (X = Cl, Br) anions in organic media. Compound **2** is converted in CH_2Cl_2: HCl(g) to $(n\text{-}Bu_4N)_2[Tc_2Cl_8]$ in ∼75% yield. We conclude that two dinuclear species with distinct bond orders (4 and 3.5) are present in the reduction product of $(n\text{-}Bu_4N)[TcOCl_4]$ with $(n\text{-}Bu_4N)BH_4$ (Tc:BH_4, 2:1). These results allowed us to simplify the preparation of $(n\text{-}Bu_4N)_2[Tc_2Cl_8]$ (Method b). The advantage of this new method is that the $(n\text{-}Bu_4N)_2[Tc_2Cl_8]$ salt can be prepared in a couple of hours (vs 3 days for the previous Method a).

C. Study of the Reaction Product of $Tc_2(O_2CCH_3)_4Cl_2$ with HCl(g) at 300 °C. Compound **3** obtained from reaction of $Tc_2(O_2CCH_3)_4Cl_2$ with HCl(g) at 300 °C is X-ray amorphous, does not contain any acetate ligands, and has a Tc content consistent with $TcCl_3$ (Experimental Section). In order to determine whether it exhibits the α-$TcCl_3$, β-$TcCl_3$, or some other structure, the compound was analyzed by EXAFS spectroscopy.

The extracted EXAFS spectrum was k^3-weighted and the FT done in the k range 2.5−14 Å^{-1}. Two different adjustments were performed considering the structure of α-$TcCl_3$ and β-$TcCl_3$.[11a,b] The scattering functions used for adjustment were calculated from the crystallographic structure of α-$TcCl_3$ and β-$TcCl_3$ (Figure 6). For adjustment, the numbers of atoms were

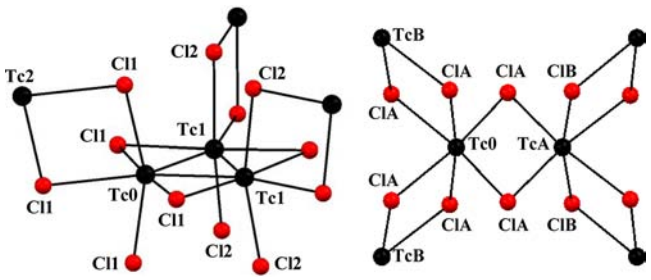

Figure 6. Ball and stick representation of the α-$TcCl_3$ (left) and β-$TcCl_3$ (right) clusters used for EXAFS calculations. Tc and Cl atoms are in black and red, respectively. Tc0 represents the absorbing atom.

fixed at those of the crystal structures; ΔE_0 was constrained to be the same value for each wave; all other parameters were allowed to vary.

The best adjustment (Figure 7, reduced chi^2 = 70) was obtained considering the structure of α-$TcCl_3$. Structural parameters (Table 5) show the presence of Tc atoms at 2.46(2) and 3.81(4) Å and of Cl atoms at 2.36(2) and 3.68(4) Å; those distances are in agreement with those found in the crystallographic structure of α-$TcCl_3$.[11a]

Adjustment considering the structure of β-$TcCl_3$ (reduced chi^2 = 95) leads to Tc−Tc distances (2.79(3) and 3.75(4) Å) that are significantly different than those reported for β-$TcCl_3$ (i.e., 2.861(2) and 3.601(2) Å). In this adjustment (Figure S6 and Table S3, Supporting Information), the DWF behave abnormally as they decrease with increasing distance.

In summary, the structural parameters obtained by EXAFS for product **3** are consistent with the X-ray structure of α-$TcCl_3$. Under these experimental conditions, the behavior of $Tc_2(O_2CCH_3)_4Cl_2$ mimics that of its Re congener but leaves unanswered the question how incipient "M_2Cl_6" rearranges to M_3Cl_9.[28] As mentioned above, Re_3Cl_9 has been widely used as precursor in the synthesis of other molecular complexes with the triangular $[Re_3]^{9+}$ core; it is expected that amorphous α-$TcCl_3$ should also lead to formation of similar complexes. In

dx.doi.org/10.1021/ic3014859 | Inorg. Chem. 2012, 51, 9563−9570

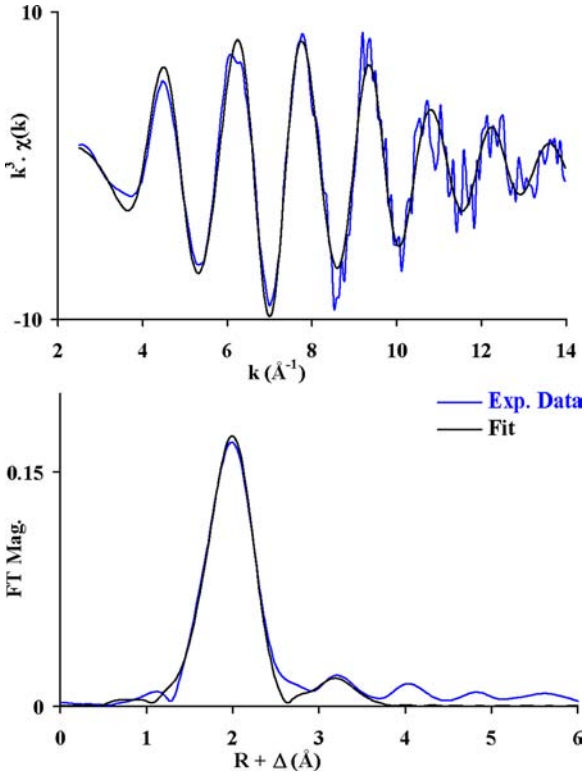

Figure 7. Fits of the experimental k^3 EXAFS spectra (top) and Fourier transform of k^3 EXAFS spectra (bottom) for compound **3** obtained from reaction of $Tc_2(O_2CCH_3)_4Cl_2$ with HCl(g) at 300 °C. Adjustment performed between k = 2.5 and 14 Å^{-1} considering the structure of α-$TcCl_3$. Experimental data are in blue, and the fit is in black.

Table 5. Structural Parameters Obtained by Adjustment of the k^3 EXAFS Spectra of Compound 3 Obtained from the Reaction of $Tc_2(O_2CCH_3)_4Cl_2$ with HCl(g) at 300 °C[a]

scattering	CN	R (Å)	σ^2 (Å^2)
Tc0 ⇆ Cl1	5	2.36(2), *2.388(4)*	0.0056
Tc0 ⇆ Tc1	2	2.46(2), *2.4445(7)*	0.0046
Tc0 ⇆ Cl2	4	3.68(4), *3.614(4)*	0.0083
Tc0 ⇆ Tc2	1	3.81(4), *3.852(1)*	0.0130

[a]Adjustment between k = 2.5 and 14 Å^{-1} considering the structure of α-$TcCl_3$. ΔE_0 (eV) = 2.29 eV. Reduced chi^2 = 70. Values found by single-crystal XRD in α-$TcCl_3$ are in italics.

this context, we find that amorphous α-$TcCl_3$ is highly soluble in concentrated aqueous HCl. Efforts are underway to isolate crystalline products from these solutions.

CONCLUSION

In summary, EXAFS spectroscopy has been used to probe the presence of metal−metal bonding in the $[Tc_2X_8]^{3-}$ (X = Cl, Br) anions, the reduction product(s) of the reaction of (n-Bu_4N)$[TcOCl_4]$ with (n-Bu_4N)BH_4 in THF, and the product obtained from reaction of $Tc_2(O_2CCH_3)_4Cl_2$ with HCl(g) at 300 °C.

For the first time, the $[Tc_2X_8]^{3-}$ anions were characterized by EXAFS spectroscopy. Structural parameters are in good agreement with those found previously by XRD techniques. As expected, the Tc−Tc separations found by EXAFS in these anions are shorter than those found in the quadruply bonded dinuclear species. EXAFS study on the oily product obtained from the reduction product of (n-Bu_4N)$[TcOCl_4]$ with (n-Bu_4N)BH_4 indicates the presence of multiple Tc−Tc-bonded dinuclear species. Attempts to isolate these species from the oily product lead to a yellow-green solid, which is also directly obtained as a precipitate during reduction of (n-Bu_4N)-$[TcOCl_4]$. Spectroscopic and XRD characterization of this solid is consistent with the presence of $[Tc_2Cl_8]^{n-}$ species (n = 2, 3). The yellow-green solid can be converted in high yield to (n-Bu_4N)$_2[Tc_2Cl_8]$. From these results, a new preparation of (n-Bu_4N)$_2[Tc_2Cl_8]$ was developed. During preparation of (n-Bu_4N)$_2[Tc_2Cl_8]$, excessive reduction of the $[TcOCl_4]^-$ anion is likely to be the reason for the low yields previously obtained. Current work is focused on using different (n-Bu_4N)$[TcOCl_4]$:(n-Bu_4N)BH_4 ratios to optimize the yield. In this context, recent results indicate that reaction of (n-Bu_4N)$[TcOCl_4]$ with (n-Bu_4N)BH_4 at 1:1 lead to (n-Bu_4N)$_2[Tc_2Cl_8]$ in ∼45% yield.

EXAFS characterization of the product obtained from reaction of $Tc_2(O_2CCH_3)_4Cl_2$ with HCl(g) at 300 °C indicates the presence of amorphous α-$TcCl_3$. The Tc−Tc separation measured in this compound is consistent with the presence of a Tc═Tc double bond in the $[Tc_3]^{9+}$ core. We hope that these new insights on the synthetic chemistry of (n-Bu_4N)$_2[Tc_2Cl_8]$ and α-$TcCl_3$ will contribute to further developments of Tc metal−metal-bonded chemistry.

ASSOCIATED CONTENT

Supporting Information

Additional synthetic details, spectroscopic characterization (EXAFS, UV−vis, IR, EDX), crystallographic tables, and X-ray crystallographic data in CIF format. This material is available free of charge via the Internet at http://pubs.acs.org.

AUTHOR INFORMATION

Corresponding Author

*E-mail: poineauf@unlv.nevada.edu.

Notes

The authors declare no competing financial interest.

ACKNOWLEDGMENTS

Funding for this research was provided by an NEUP grant "Development of Alternative Technetium Waste Forms" from the U.S. Department of Energy, Office of Nuclear Energy, through INL/BEA, LLC, 89445. Use of the Advanced Photon Source at Argonne was supported by the U.S. Department of Energy, Office of Science, Office of Basic Energy Sciences, under Contract No. DE-AC02-06CH11357. The authors thank Trevor Low and Julie Bertoia for outstanding health physics support and Dr. Sungsik Lee at the APS for expert technical assistance during the EXAFS experiments.

REFERENCES

(1) (a) Cotton, F. A.; Murillo, C. A.; Walton, R. A. In *Multiple Bonds between Metal Atoms*, 3rd ed.; Cotton, F. A., Murillo, C. A., Walton, R. A., Eds.; Springer: New York, 2005; Chapter 1. (b) Canterford, J. H.; Colton, R. *Halides of the Second and Third Row Transition Metals*; John Wiley and Sons: New York, 1968. (c) Cotton, F. A.; Wilkinson, G.; Murillo, C. A.; Bochmann, M. *Advanced Inorganic Chemistry*, 6th ed.; John Wiley and Sons: New York, 1999. (d) Shtemenko, N.; Collery, P.; Shtemenko, A. *Anticancer Res.* **2007**, *27*, 2487−2492. (e) Hogarth, G. *Organomet. Chem.* **1995**, *24*, 184−232. (f) Timmons, D. J.; Doyle, M. P. In *Multiple Bonds between Metal Atoms*, 3rd ed.; Cotton, F. A., Murillo, C. A., Walton, R. A., Eds.; Springer, New York, 2005; Chapter

13. (g) Muetterties, E. L.; Krause, M. J. *Angew. Chem., Int. Ed.* **1983**, *22*, 135−148.
(2) (a) Berry, J. F. In *Multiple Bonds between Metal Atoms*, 3rd ed.; Cotton, F. A., Murillo, C. A., Walton, R. A., Eds.; Springer, New York, 2005; Chapter 15. (b) Chisholm, M. H.; Macintosh, A. M. *Chem. Rev.* **2005**, *105*, 2949−2976. (c) Lin, J.; Miller, G. J. *Inorg. Chem.* **1993**, *32*, 1476−1487. (d) Walton, R. A. In *Multiple Bonds between Metal Atoms*, 3rd ed.; Cotton, F. A., Murillo, C. A., Walton, R. A., Eds.; Springer: New York, 2005; Chapter 8. (e) Thimmappa, B. H. S. *Coord. Chem. Rev.* **1995**, *143*, 1−34.
(3) (a) Bertrand, J. A.; Cotton, F. A.; Dollase, W. A. *Inorg. Chem.* **1963**, *6*, 1166−1171. (b) Cotton, F. A.; Harris, C. B. *Inorg. Chem.* **1965**, *4*, 330−333.
(4) Barder, T. J.; Walton, R. A. *Inorg. Chem.* **1982**, *21*, 2510−2511.
(5) Walton, R. A. *J. Cluster Sci.* **2004**, *15*, 559−588.
(6) Sattelberger, A. P. In *Multiple Bonds between Metal Atoms*, 3rd ed.; Cotton, F. A., Murillo, C. A., Walton, R. A., Eds.; Springer: New York, 2005; Chapter 7.
(7) (a) Poineau, F.; Gagliardi, L.; Forster, P. M.; Sattelberger, A. P.; Czerwinski, K. R. *Dalton Trans.* **2009**, *30*, 5954−5959. (b) Poineau, F.; Forster, P. M.; Todorova, T. K.; Gagliardi, L; Sattelberger, A. P.; Czerwinski, K. R. *Dalton Trans.* **2012**, *41*, 2869−2872. (c) Poineau, F.; Forster, P. M.; Todorova, T. K.; Gagliardi, L.; Sattelberger, A. P.; Czerwinski, K. R. *Inorg. Chem.* **2010**, *49*, 6646−6654.
(8) (a) Poineau, F.; Sattelberger, A. P.; Conradson, S. D.; Czerwinski, K. R. *Inorg. Chem.* **2008**, *47*, 1991−1999. (b) Poineau, F.; Sattelberger, A. P.; Czerwinski, K. R. *J. Coord. Chem.* **2008**, *61*, 2356−2370.
(9) Preetz, W.; Peters, G. *Z. Naturforsch.* **1980**, *35B*, 797−801.
(10) (a) Preetz, W.; Peters, G.; Bublitz, D. *J. Cluster Sci.* **1994**, *5*, 83−106. (b) Cotton, F. A.; Daniels, L.; Davison, A.; Orvig, C. *Inorg. Chem.* **1981**, *20*, 3051−3055. (c) Schwochau, K.; Hedwig, K.; Schenk, H. J.; Greis, O. *Inorg. Nucl. Chem. Lett.* **1977**, *13*, 77−80.
(11) (a) Poineau, F.; Johnstone, E. V.; Weck, P. F.; Kim, E.; Forster, P. M.; Scott, B. L.; Sattelberger, A. P.; Czerwinski, K. R. *J. Am. Chem. Soc.* **2010**, *132*, 15864−15865. (b) Poineau, F.; Johnstone, E. V.; Weck, P. F.; Forster, P. M.; Kim, E.; Czerwinski, K. R.; Sattelberger, A. P. *Inorg. Chem.* **2012**, *51*, 4915−4917. (c) Poineau, F.; Malliakas, C. D.; Weck, P. F.; Scott, B. L.; Johnstone, E. V.; Forster, P. M.; Kim, E; Kanatzidis, M. G.; Czerwinski, K. R.; Sattelberger, A. P. *J. Am. Chem. Soc.* **2011**, *133*, 8814−8817.
(12) Johnstone, E. V.; Poineau, F.; Forster, P. M.; Ma, L.; Hartmann, T.; Cornelius, A.; Antonio, D.; Sattelberger, A. P.; Czerwinski, K. R. *Inorg. Chem.* **2012**; http://dx.doi.org/10.1021/ic301011c.
(13) Esjornson, S. M. V.; Fanwick, P. E.; Walton, R. A. *Inorg. Chim. Acta* **1989**, *162*, 165−166.
(14) The position of the absorption edge for $Tc_2X_8^{3-}$ (21 050.6 eV for X = Cl and 21 049.8 eV for X = Br) is lower than the one reported for $Tc_2X_8^{2-}$ (21 052 eV for X = Cl and 21 051 eV for X = Br) and consistent with an average oxidation state of +2.5 of the Tc atoms. UV−visible spectra of the $Tc_2X_8^{3-}$ species in concentrated HX exhibit the characteristic bands at 15 760 cm^{-1} for X = Cl and 14 409 cm^{-1} for X = Br.
(15) Beno, M. A.; Engbretson, M.; Jennings, G.; Knapp, G. S.; Linton, J.; Kurtz, C.; Rutt, U.; Montano, P. A. *Nucl. Instrum. Methods A* **2001**, *467−468*, 699−702.
(16) Ravel, B.; Newville, M. *J. Synchrotron Radiat.* **2005**, *12*, 537−541.
(17) Ressler, T. *J. Synchrotron Radiat.* **1998**, *5*, 118−122.
(18) Rehr, J. J.; Albers, R. C. *Rev. Mod. Phys.* **2000**, *72*, 621−654.
(19) Ravel, B. *J. Synchrotron Radiat.* **2001**, *8*, 314−316.
(20) (a) Sheldrick, G. M. *Acta Crystallogr., Sect. A* **2008**, *64*, 112−122. (b) Dolomanov, O. V.; Bourhis, L. J.; Gildea, R. J.; Howard, J. A. K.; Puschmann, H. *J. Appl. Crystallogr.* **2009**, *42*, 339−341.
(21) Koyama, M.; Kanchiku, Y.; Fujinaga, T. *Coord. Chem. Rev.* **1968**, *3*, 285−291.
(22) Cotton, F. A.; Shive, L. W. *Inorg. Chem.* **1975**, *14*, 2032−2035.
(23) Faggiani, R.; Lock, C. J. L.; Poce, J. *Acta Crystallogr.* **1980**, *B36*, 231−233.
(24) Schwochau, K. *Technetium: Chemistry and Radiopharmaceutical Applications*; Wiley-VCH: Weinheim, Germany, 2000; pp 313−314.
(25) (a) Yegen, E.; Hagenbach, A.; Abram, U. *Chem. Commun.* **2005**, *44*, 5575−5577. (b) Hagenbach, A.; Yegen, E.; Abram, U. *Inorg. Chem.* **2006**, *45*, 7331−7338. (c) Cotton, F. A.; Davison, A.; Day, V, W.; Gage, L. D.; Trop, H. S. *Inorg. Chem.* **1979**, *18*, 3024−3029.
(26) Clarke, M. J.; Kastner, M. E.; Podbielski, L. A.; Fackler, P. H.; Schreifels, J.; Meinken, G.; Srivastava, S. C. *J. Am. Chem. Soc.* **1988**, *110*, 1818−1827.
(27) (a) Cotton, F. A.; Haefner, S. C.; Sattelberger, A. P. *Inorg. Chem.* **1996**, *35*, 1831−1838. (b) Cotton, F. A.; Fanwick, P. E.; Gage, L. D.; Kalbacher, B.; Martin, D. S. *J. Am. Chem. Soc.* **1977**, *99*, 5642−5645.
(28) Glicksman, H. D.; Hamer, A. D.; Smith, T. J.; Walton, R. A. *Inorg. Chem.* **1976**, *15*, 2205−2209.